Pergamon

Int. J. Heat Mass Transfer. Vol. 39, No. 17, pp. 3749–3759, 1996

0017-9310/96 $15.00 + 0.00

PII: S0017-9310(96)00017-8

Natural convection in a liquid metal enclosure with floor cooling

A. W. STEVENS

BNFL Engineering Ltd, The Victoria, Harbour City, Salford Quays, Manchester M5 2SP, U.K.

(*Received* 14 *June* 1993 *and in final form* 6 *February* 1995)

Abstract—Temperature measurements made in an annular, sodium filled enclosure heated at the inner wall or the roof boundary and cooled at the floor are reported. The dimensionless temperature profile of the bulk fluid in response to uniform wall heating is described by an empirical formula, which is the Fourier linear conduction equation with an additional simple function accounting for convection. The formula is subsequently shown to be a solution of the one-dimensional steady-state conduction equation involving energy generation in the medium. The analytical approach enables the convection and conduction heat transfer modes in the bulk fluid to be isolated and hence, the convection currents to be quantified. Copyright © 1996 Elsevier Science Ltd.

1. INTRODUCTION

The study of natural convection in enclosures containing a liquid metal has been researched in the nuclear industry in recent years to provide design data for liquid metal cooled fast breeder reactors (LMFBR's).

This paper reports some experimental observations and analysis made in sodium on the enclosure representing the intermediate plenum of a UK Design of LMFBR. This is an annular space around the reactor core filled with sodium. Its intention is to hold a stagnant stratified sodium layer and to limit the temperature gradient between the hot pool above and the cooler sodium pool below. Since one boundary is a vertical wall adjacent to the reactor core, then heat on this wall could cause naturally convected sodium movement which may destroy the stratification in the bulk sodium. This might create unacceptable temperature gradients. Concerns about the influence of this heated vertical wall were the main drivers for the test work.

Work on this subject has been published previously which gives fuller descriptions of the plenum and also include results made in earlier test rigs using initially water and later mercury as the simulant reactor fluid [1, 2].

The purpose of this paper is to report the sodium experimental results and to introduce the empirical and analytically derived formulae that enable the steady-state temperature distribution and the fluid flow within the enclosure to be predicted. The formulae could be used in simple geometries and possibly extended to more complex shapes and other fluids. The structural design of such enclosures can then proceed with more confidence.

2. THE TEST FACILITY

Figure 1 schematically illustrates the test vessel which models the intermediate plenum. The preliminary data for this design were obtained from a simple rectangular tank filled with mercury [2]. The data provided a useful comparison with these results and are reported later.

The test section was large, being nearly 1 m high and forming an annulus between a central column (600 mm diameter) and the outer cylinder (1800 mm

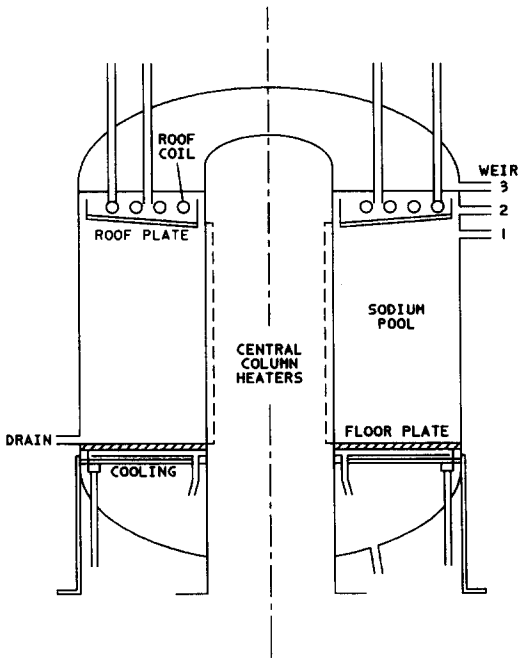

Fig. 1. Schematic arrangement of the test vessel.

NOMENCLATURE

A area [m^2]
$C_{1,2}$ integration constants
C_p specific heat [J kg^{-1} K^{-1}]
g_0 constant energy generation [W m^{-3}]
k thermal conductivity [W m^{-1} K^{-1}]
h heat transfer coefficient [W m^{-2} K^{-1}]
H height of heated wall [m]
H' height of heated wall to the roof boundary condition [m]
H_0 height of uniformly heated wall with an adiabatic top boundary i.e. reference height [m]
(H) dimensionless temperature $= \dfrac{T-T_c}{T_h-T_c}$
m' mass flow [kg s^{-1}]
Pe Peclet number
Q total heat flow [W]
Q_c conduction heat [W]
Q_{cv} convection heat [W]
Q_r roof heat [W]
Q_t total heat [W]
Q_w wall heat [W]
R heat ratio
T local temperature [K]
T_h hottest temperature [K]
T_c floor or sink temperature [K]
T_∞ temperature at infinity, equal to T_c [K]
T^* dimensionless temperature $= \dfrac{kA}{QH}(T-T_c)$
U downward convection velocity in the bulk fluid [m s^{-1}]
z local height [m]
z^* dimensionless height parameter $[z/H_0]$.

Greek symbols

α thermal diffusivity $= \dfrac{k}{\rho \cdot C_p}$ [m^2 s^{-1}]
ρ density [kg m^{-3}].

diameter). When full the vessel contained approximately two tonnes of sodium. The central column or inner wall simulated the reactor core as the prime source of heat. This heat source was divided into 10 equal horizontal zones by 10 band heaters mounted behind the wall of the central column and independently powered and controlled. These 10 zones provided flexibility in the heat pattern applied to the wall, which could be varied from constant heat flux to cases of nonuniform flux.

The floor plate was cooled from below using sodium, which circulated within a labyrinth designed specifically to provide a uniform floor temperature (i.e. simulating the cold pool boundary).

The level of sodium in the annular section could be adjusted in increments to correspond with the submergence of a number of heater zones. In some tests the top boundary was a free surface to an argon gas cover blanket which formed an adiabatic thermal boundary. As the level of sodium was raised further it covered an internal baffle and flooded the region around the roof coil. The top could then be heated from a stream of sodium in the coil and the test conditions changed to those involving a heated roof (i.e. simulating the hot pool boundary).

The outer vertical wall of the vessel was guard heated for all tests and represented an adiabatic thermal boundary.

The temperature monitoring instrumentation consisted of fixed positions of thermocouples mounted as indicated in Fig. 2.

- Six equally spaced columns for bulk sodium measurements positioned to have an equal volume of sodium either side to the walls (i.e. the pool tree thermocouples);
- three columns for wall temperature data on both the inner and outer vessel walls;
- combs protruding horizontally from the inner wall at a quarter height (236 mm) and three-quarter height (700 mm) above the floor plate to give data on the thermal boundary region. These were placed at 5 mm intervals to a distance of 60 mm from the wall and are based on measurements made and reported in ref. [3].

Input heat was measured as the electrical power applied to the column heaters, and output heat from a calculation using the measured temperature differential across the floor plate. The thermocouples and heat fluxes through the floor plate were initially calibrated in a series of stable linear conduction tests where heat was introduced via the roof coil and removed at the floor. Careful calculations of heat balances ensured that the main heat flows were quantified.

The stabilization period before taking the steady-state temperature data was generally 24 h.

3. RESULTS OF EXPERIMENTS

3.1. *Main tests. Uniform wall heat flux applied to the central column, adiabatic roof, cooled floor*

These results record the temperature stratification in the pool when heat was applied uniformly to the central column for the full height of sodium. Tests were made at four sodium levels and three input heat fluxes per height variant over the range 10–22 kW m^{-2}.

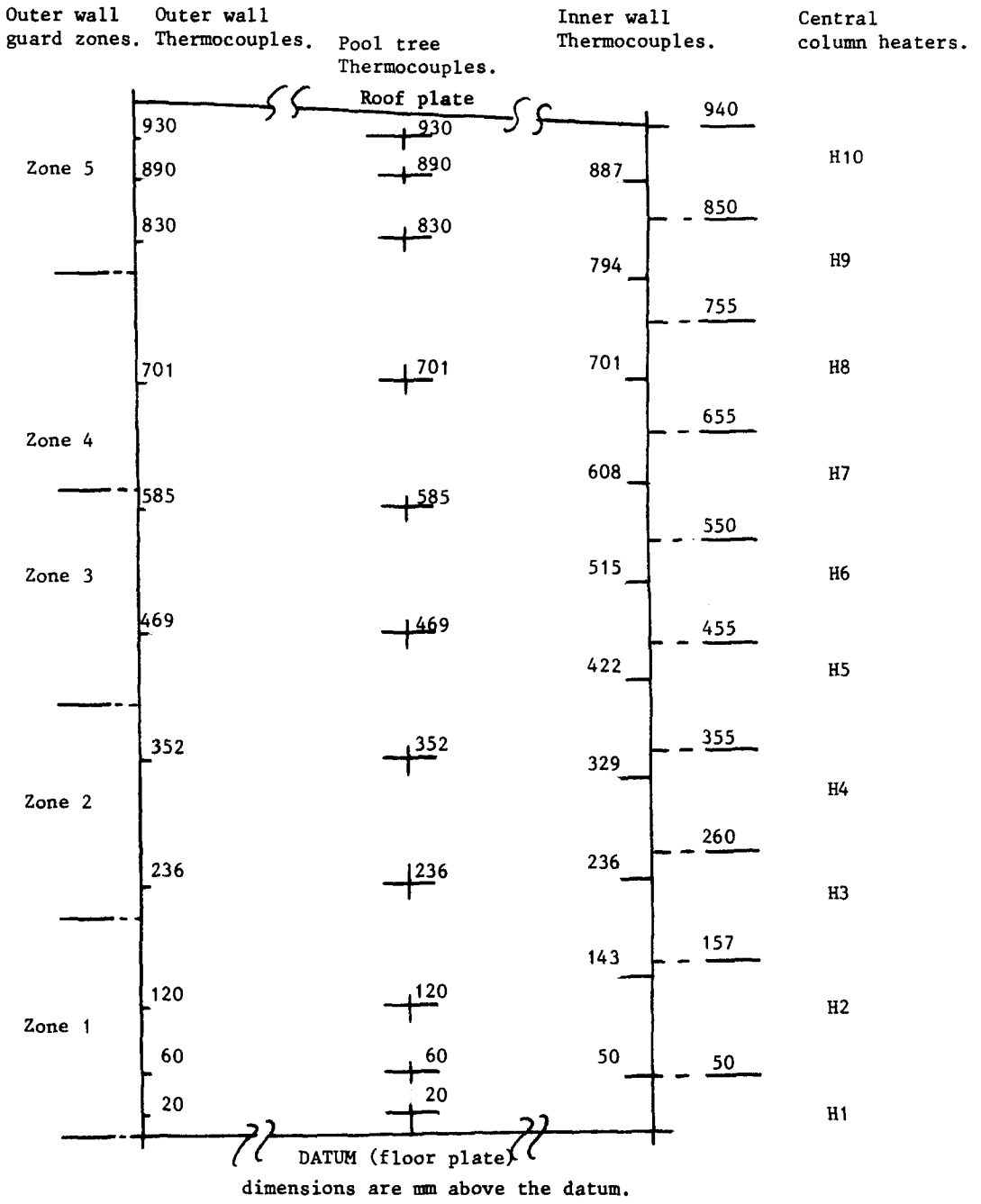

Fig. 2. Pool section showing relative positions of heaters and thermocouples.

The top of the pool was adiabatic to a free surface and the outer wall also adiabatic. The floor was cooled.

Table 1 summarizes the depth of sodium heated on the inner central column against an aspect ratio defined as the heated wall area divided by the cooled floor plate area.

The results are shown on Figs. 3 and 4, and are presented in dimensionless format to show the bulk temperature profile from the floor to the free surface. Actual temperatures ranged from 280°C at the floor to 390°C at the top of the sodium.

Table 1.

Number of submerged vertical wall heaters	Depth of sodium equal to the heated wall height (mm)	Aspect ratio $\frac{\text{(heated wall area)}}{\text{(cooled floor area)}}$
4	360	0.30
6	550	0.46
8	775	0.65
10	940	0.79

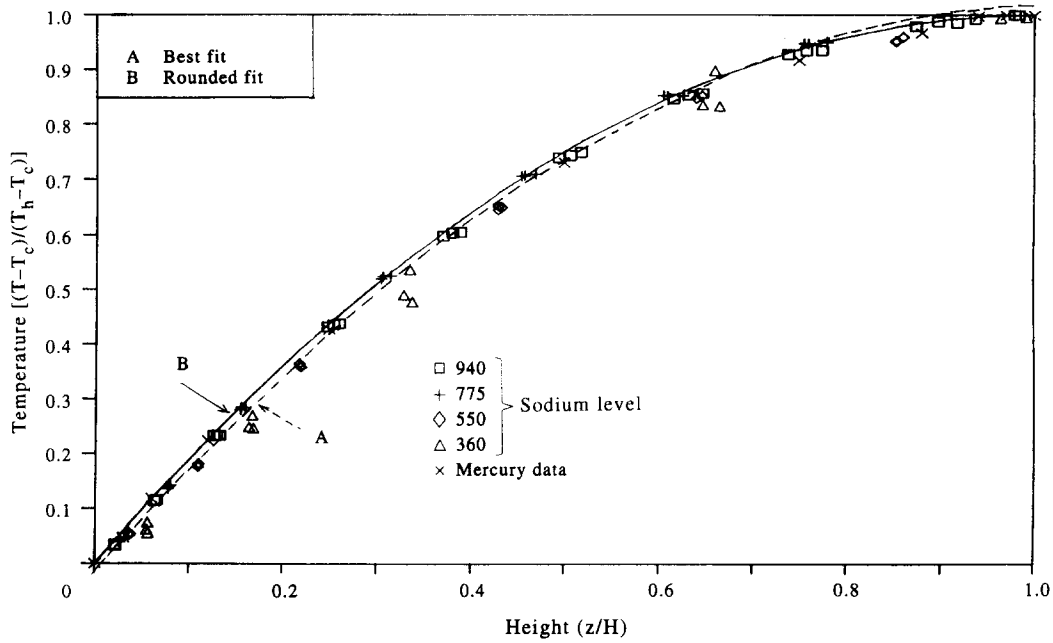

Fig. 3. Normalized pool temperature for uniform wall heating (plot 1).

The dimensionless parameters are:
Dimensionless height (abscissa)

$$z^* = \frac{z}{H}. \tag{1}$$

Dimensionless temperature (ordinate)

$$\text{either (Fig. 3) } (H) = \frac{T - T_c}{T_h - T_c} \tag{2}$$

or for an alternative plot (Fig. 4)

$$T^* = \frac{kA(T - T_c)}{QH}. \tag{3}$$

Figure 3 also includes some of the mercury rig data obtained from the authors of the work on a rectangular mercury filled enclosure [2]. The size of that enclosure had a heated side wall 0.28×0.30 m and a cooled floor 0.6×0.28 m.

The experimental observations were:

(1) Temperatures across horizontal planes in the

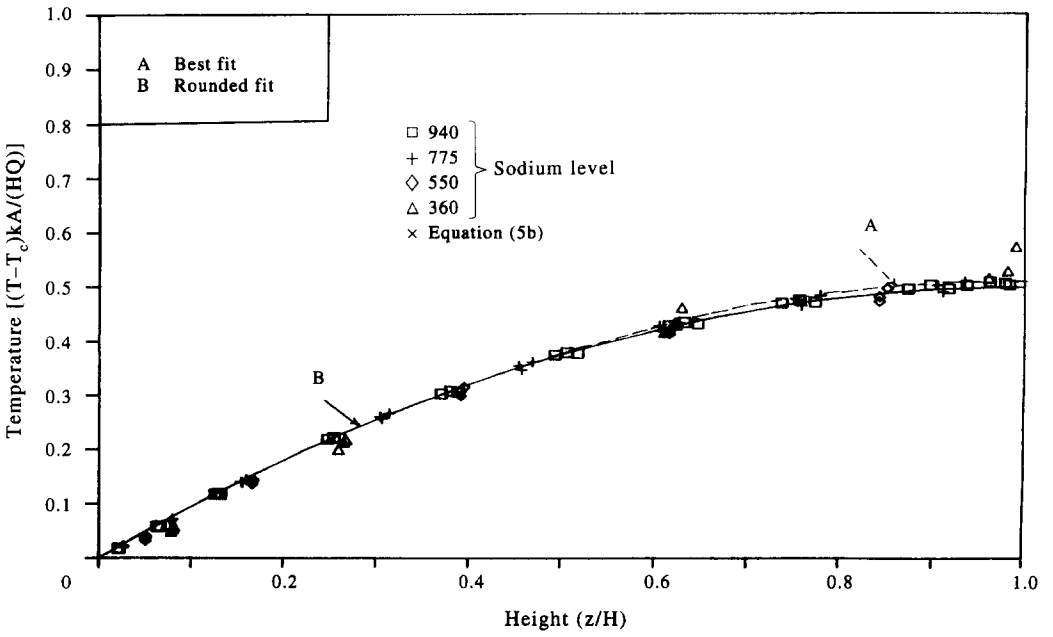

Fig. 4. Normalized pool temperature for uniform wall heating (plot 2).

vessel were constant. This confirmed the temperature stratification and a one-dimensional temperature profile through the bulk sodium from the top of the enclosure to the floor.

(2) The results covered aspect ratios ranging from 0.3 to 0.8 and showed no sensitivity to this aspect parameter.

(3) Within this aspect ratio range were the conditions represented by the mercury experiments [2] (i.e. aspect ratio = 0.5). These agreed well with the sodium results. Thus liquid metals with Prandtl numbers of 0.005 for sodium and 0.025 for mercury showed good agreement.

(4) The normalized temperature profile was independent of applied power (for the range tested).

(5) The profile, which is presented in Fig. 3, could best be represented by the following curve obtained by applying multiple regression analysis to all the experimental results.

$$(H) = -0.01 + 1.96z^* - 0.93(z^*)^2. \quad (4a)$$

Ignoring the intercept coefficient which is clearly an error, and rounding-off the coefficients to satisfy the boundary conditions suggests that the profile may be expressed by a quadratic which also provides a good fit (also shown in Fig. 3)

$$(H) = 2z^* - (z^*)^2. \quad (4b)$$

Figure 4 shows the results from the sodium data by plotting dimensionless height [equation (1)] against temperature [equation (3)].

The observations are similar to those drawn above, with the dimensionless temperature profile being expressed by a best fit quadratic curve as follows:

$$T^* = -0.006 \times 1.019(z^*) - 0.495(z^*)^2. \quad (5a)$$

When the coefficients are rounded to whole numbers the following is obtained:

$$T^* = z^* - \tfrac{1}{2}(z^*)^2. \quad (5b)$$

3.2. *Uniform wall heating and a heated roof*

Further experiments were also made using the additional variant of roof heating, as well as heat applied to the central column. To achieve this the sodium level was raised to cover the roof coil.

Figures 5 and 6 show the dimensionless temperature profiles when heat was applied either completely at the roof or uniformly to the central column. Two further tests show intermediate positions where a combination of both were used (i.e. 46 and 9% roof heating). All heat was removed at the floor. The rounded-off curves derived in the previous section for uniform wall heat only, were also included on Figs. 5 and 6.

The straight line on both figures represented the linear conduction of heat from the roof to the floor without any wall heating. Such tests are typical of those used to calibrate the floor plate as a heat flux meter.

The dimensionless format shown in Fig. 5 is a conventional way of presenting the experimental results and useful in comparing different heat patterns. However the presentation of Fig. 6 appears to be more informative in explaining the heat transfer mechanisms taking place in the enclosed pool. It shows the Fourier equation for linear conduction (i.e. the straight line) as a basis for comparison at one extreme. The other extreme is given by uniform sidewall heating

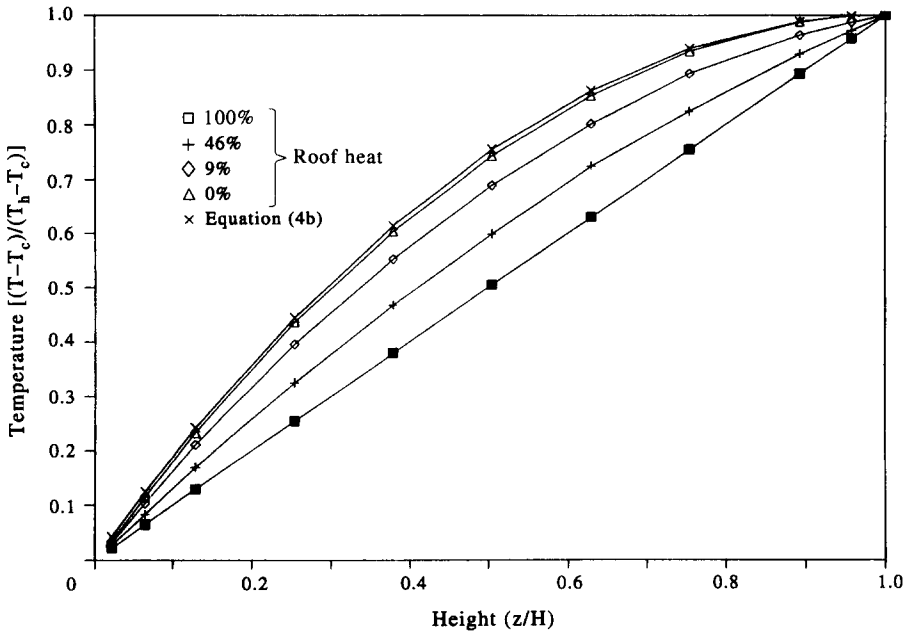

Fig. 5. Normalized pool temperature for uniform wall heating and/or a heated roof (plot 1).

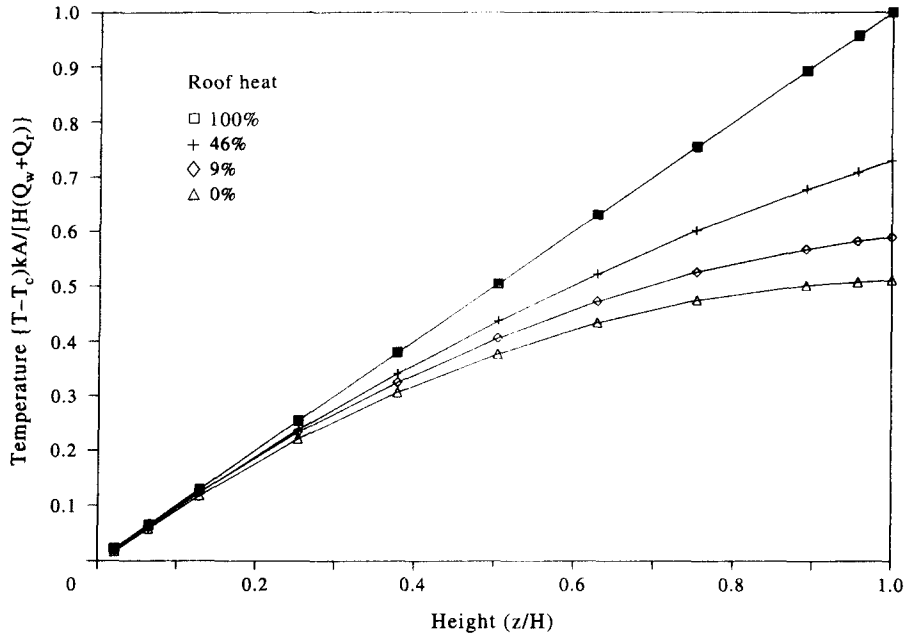

Fig. 6. Normalized pool temperature for uniform wall heating and/or a heated roof (plot 2).

only (i.e. initial convection only) with intermediate positions showing a combination of these two mechanisms.

The further interesting observations noted were:

- all the plots on Fig. 6 tended to the same gradient as the linear conduction tests at the floor, confirming that conduction only was the mechanism for heat transfer out of the pool irrespective of the heating pattern;
- stirring of the pool by the sidewall induced natural convection currents halved the temperature potential needed to transfer the same quantity of heat as was necessary for conduction from the roof boundary alone (Fig. 6).

Hence, some significance can now be placed on the terms in equation (5b). The first term appears to define the conduction down the pool only, whereas the second term on the right hand side identified as

$$-\tfrac{1}{2}(z^*)^2 \qquad (6)$$

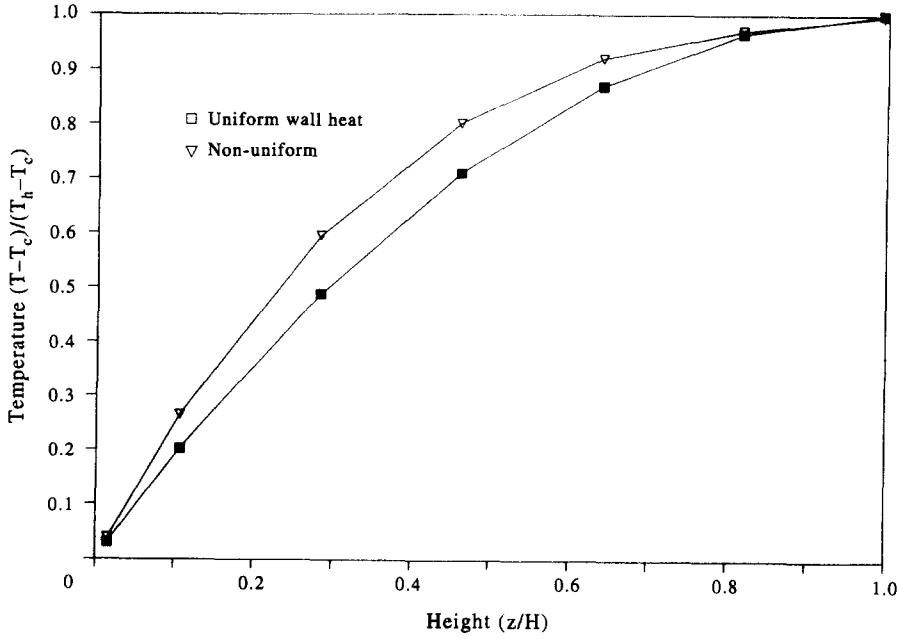

Fig. 7. Normalized temperature profile for nonuniform vs uniform wall heating.

probably accounts for the convection induced by the sidewall. At the base when z^* is small the influence of this term is negligible, but because of the square function its influence increases markedly until it dominates at the top of the natural convection region. Here the parameter z/H tends to a value of one and the net temperature gradient given by equation (5) is halved. This is consistent with the empirical observations [2] when it was concluded that natural convection was doubling the heat transfer rate from the fluid to the base for the same overall temperature potential.

3.3. *Local uniform wall heating*

It was possible, because of the size of the test facility, to apply uniform wall heating to a local section and still obtain good resolution of the bulk sodium temperature profile. Thus, heat was applied uniformly to a block of four adjacent heater zones and only the height of this block above the floor altered between each test.

No graphical illustrations of the tests are given, since it was found that the same one-dimensional shape for the temperature profile was obtained, provided the results were normalized to specific parameters. These parameters could be isolated within the geometry of the test facility and are identified in the results described as follows:

(1) Curvature in the temperature field occurred in the sodium only at heights directly adjacent to the applied heat on the wall. Thus the one-dimensional temperature profile was divided into three regions.

(a) A zone beneath the heated wall with a linear straight line gradient indicative of conduction and as observed only in the heated roof tests.

(b) A curvature zone adjacent to the heated wall of the shape seen in Figs. 3 and 4, provided the data was normalized to the parameters of the temperatures at the top and bottom of the heated region (i.e. T_h and T_c) and H taken as the heated height.

(c) An isothermal zone above the heated wall and consistent with the top adiabatic boundary for the pool.

(2) If the heated block was positioned higher in the pool then the conduction zone was thicker and the top temperature correspondingly higher. Applied heat and sink temperatures were unchanged.

(3) Significantly there appeared to be little or no heating of the pool by the thermal convection current once it rose above the heated wall.

(4) The change in the top of the heated boundary from a free surface to an interface within the sodium did not appear to alter the shape of the bulk fluid temperature field adjacent to the uniformly heated wall.

These observations indicated firstly, that curvature of the temperature field was confined to the level at which power was applied on the sidewall. Such an observation is consistent with the generation of internal heat in the heated band, and this will be developed further in Section 4.

Secondly, that a height parameter had been isolated for this generation zone which corresponded to the height of the heated wall.

3.4. *Tests with nonuniform wall heating*

Two further test types were undertaken to give an indication of the changes in the heat transfer mechanisms as one moved away from the uniformly heated wall condition to more complicated and possibly more realistic problems.

3.4.1. In the first test group the heat pattern was maintained with a uniform background wall heating (as previously), but with an additional variant of extra uniform heating on a two heater block which was six times the background heat flux (i.e. a local hot band). This local hot band was positioned at different heights between tests, with the total heat transferring through the pool to the floor which was kept at a constant sink temperature.

Again no graphical illustrations of the results are included, since they are very specifically related to the heat pattern chosen, but one further interesting observation was confirmed:

Additional steepening of the one-dimensional temperature field occurred only adjacent to the height that corresponded to the extra heated area of the wall. This clearly related extra power on the sidewall with the additional temperature difference in the bulk sodium, i.e. further confirmation of the appearance of energy generation in the bulk fluid.

3.4.2. The second group of tests were made with a heat pattern that concentrated the power input towards the base of the pool in an attempt to achieve results similar to those observed in the water tests with an isothermal wall [1]. The temperature profiles obtained are again specific to the heat pattern applied. The choice was arbitrary, but in this case the heat was distributed over six heaters as

		%
Top heater	6	5
	5	10
	4	15
	3	20
	2	25
	1	25
		100

The dimensionless profile is shown on Fig. 7 and compared with that for uniform wall heating. The length dimension is normalized to the heated height.

The concentration of heat towards the floor produced a steeper temperature gradient again in response to the power distribution on the wall. By choosing alternative heat patterns with even more wall heating towards the base, then probably it would be possible to simulate the temperature profiles observed in water experiments with an isothermal wall [1]. This

was not possible in this rig because of the risk of exceeding the safe stress limit.

3.5. *Boundary layer observations*

Observations from the thermocouple combs adjacent to the hot wall for a sodium depth of 940 mm, showed that the temperature field was very thin and that the boundary layer difference between the hot wall and the bulk sodium was small.

At the lower position (height 236 mm), this temperature difference was less than 0.5% of that between the top and floor of the pool. The observed thickness as measured by the thermocouple combs described in Section 2 was less than 5 mm. At the higher position of three-quarters height (700 mm) the wall/pool difference locally was less than 2% and the thickness about 12 mm. These are considerably thinner than predicted by previous correlations [3]. The reason for this difference is not known, but it could be a consequence of the stratification of the sodium in the enclosure which prevents the boundary layer fully developing. As the hot sodium rises it moves into equally hot fluid and the buoyancy driving forces may be destroyed on the outer edge of the velocity boundary layer.

These results confirmed the assumptions used in developing a previous analytical solution [2], and which were important in justifying the one-dimensional theory, i.e.

- that it is reasonable to assume that the wall temperature excess above the bulk temperature is small;
- that the thermal boundary layer is thin.

4. DISCUSSION OF RESULTS AND ANALYSIS

4.1. *Empirical formulae*

The empirical equations (4) and (5), presented earlier for constant wall heating, are shown both as the best fit regression lines of an assumed quadratic function and also rounded-off to whole numbers to satisfy expected boundary conditions at the top boundary (i.e. adiabatic) and at the floor (i.e. conduction only).

Any deviation of the top gradient from zero would be attributed to the excess temperature in the thermal circulation up the heated wall. This excess could represent heat spread out across the free surface and could give an apparent top heating similar to the tests when the roof was deliberately heated. If one evaluated the gradient at the top using the best fit constants for equation (4a) it would give a value of 0.1 or 5% of the floor gradient and for equation (5a) 2.8% of the floor gradient. Hence, there is some contribution from the convection mechanism against the side wall towards producing top heating.

However, it appears that in a liquid metal its influence on the top gradient is small and for most engineering applications this could initially be ignored. The experimental observations confirm this.

4.2. *Analytical formulae*

The temperature profile given by equation (5b) is a specific solution of the one-dimensional steady-state heat conduction equation involving constant energy generation in the medium [4], and the solution is demonstrated in the Appendix.

This indicates that the temperature profile in the liquid metal pool is in response to constant energy generation from the downward convection currents in the sodium, which mirror the constant heat flux applied to the vertical wall and the upward convection current in the boundary layer.

This agreement of the analytical solution with the empirically derived formula leads to further understanding of the distribution of the conduction and convection heat transfer modes in the bulk sodium and to the simplified analysis model presented in ref [2]. That model suggested a relatively thin boundary layer flow travelling up the heated wall with a balanced return flow spread across the plenum width. It appears from these tests that as the downward convective current re-entrains into the sidewall boundary layer, the termination of the flow in the bulk fluid provides the energy generation and the release of heat from the convection mode which then proceeds down the enclosure in a conduction mode. The distribution of heat by the two mechanisms is closely linked and further analytical formulae may be derived for this constant heated wall condition to explain convection heat distribution flows.

4.2.1. *Conduction heat.* The quantity of heat in the conduction mode at any height is defined by the differential of equation (5), i.e.

$$\frac{Q_c(z^*)}{Q_t} = \frac{(\mathrm{d}T^*)}{(\mathrm{d}z^*)} = 1 - z^*. \tag{6}$$

This varies from 100% at the floor, to zero at the top in a simple linear relationship.

4.2.2. *Convection heat.* The quantity of heat in the convection mode at any height is the converse being 100% at the top and reducing to zero at the floor, i.e.

$$\frac{Q_{cv}(z^*)}{Q_t} = z^*. \tag{7}$$

The total heat is constant at any height and is the sum of the local heat moving in either the conduction or convection modes. Since the convection heat is directly proportional with height, it follows that this is also the cumulative heat applied at a constant rate to the wall up to the same height.

4.2.3. *Convection flows.* The local ratio of heat in each heat transfer mode at any height defines a local Peclet no.

$$Pe(z^*) = \frac{Q_{cv}(z^*)}{Q_c(z^*)} = \frac{z^*}{1 - z^*} = \frac{\rho \cdot C_p \cdot U(z^*) \cdot A \cdot \mathrm{d}T}{kA \cdot \mathrm{d}T/H}. \tag{8}$$

From this relationship it is possible to quantify the

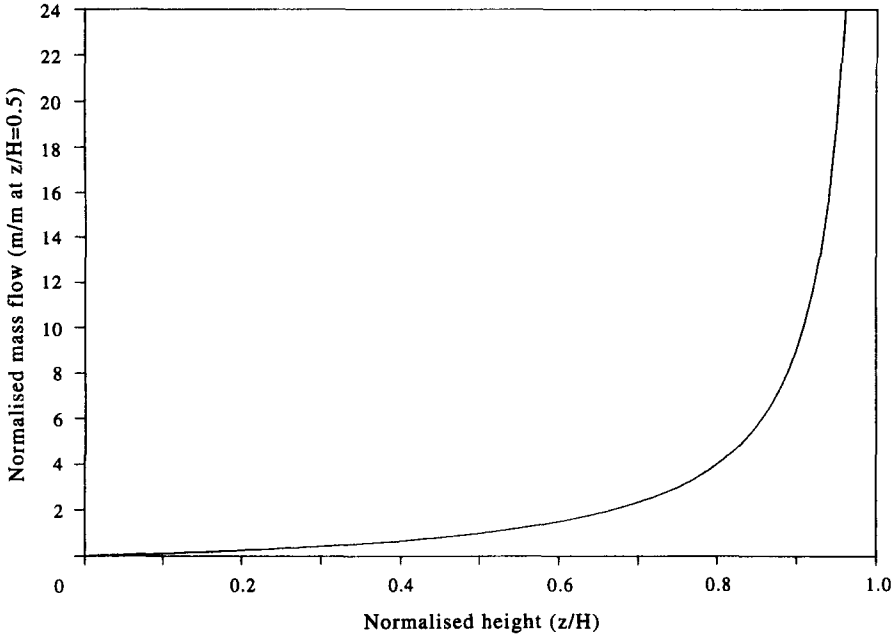

Fig. 8. Normalized mass flow in the bulk fluid.

minimum convection flows circulating in the enclosure; since mass flow at any height is given by

$$m'(z^*) = \rho \cdot U(z^*) \cdot A. \tag{9}$$

Then rearranging and introducing the thermal diffusivity yields expressions for the local mass flow in the bulk fluid down the enclosure

$$m'(z^*) = \frac{\rho \cdot A\alpha}{H}\left(\frac{z^*}{1-z^*}\right). \tag{10}$$

By virtue of continuity, this also defines the upward mass flow in the boundary layer adjacent to the heated surfaces.

Normalization of this equation to the value at mid-height simplifies this expression to give

normalized mass flow

$$\frac{m'(z^*)}{m'(z^* = 0.5)} = \frac{z^*}{1-z^*}. \tag{11}$$

Equation (11) has been solved and the result presented on Fig. 8. This indicates the relative magnitude of the convection currents in the bulk fluid with considerable recirculation at the top of the enclosure, but only drift flow downwards for much of the height. Since the above equation tends to infinity at $z^* = 1$, the influence of the boundary layer must be taken into account and hence, the data is only plotted upto $z^* = 0.975$ and thus allows for the slight top heating effect noted in the empirical equations as discussed previously.

4.3. *Analysis of a heated roof with wall heating*

The previous analysis leads to an explanation of the roof heated tests. Here heat was introduced at the roof boundary producing an initial conduction gradient. Thus equation (6) could be re-written as

$$\frac{Q_r}{Q_r + Q_w} = \left(\frac{dT^*}{dz^*}\right), \tag{12}$$

where conduction at the top boundary has been replaced by the in-flow of roof heat (Q_r) and the total heat (Q_t) by the sum of the roof heat (Q_r) and uniform wall heat (Q_w) inducing the convection. This defines the temperature gradient boundary condition at the roof level.

Roof heating in its various degrees provides a whole range of intermediate positions along the curve defined by equation (5b) and indicated by Fig. 3. This may require a tighter definition of H for the uniformly heated wall, which one has chosen to define as H_0 or reference height. This reference height is the height necessary to obtain the full development of the temperature profile curve as far as the true adiabatic boundary. Thus, for the roof heated tests (where only a limited development of the curve is seen up to a height H' representing the heated wall height to the roof boundary condition), a relationship between H_0 and H' is required. This relationship can be derived by equating equations (6) and (12) and solving when $z = H'$ so that $z^* = H'/H_0$. Thus

$$H' = \frac{Q_w}{(Q_r + Q_w)} \cdot H_0 \tag{13}$$

and the temperature field would be defined by equation (5b) solved between $z^* = 0$ to $z^* = H'/H_0$, where $H' < H_0$ and $Q = Q_t = Q_r + Q_w$.

The experimental data on Fig. 6 was plotted for z/H' in the range 0 to 1. To obtain the equation of the

line based on normalization to the heated wall height requires substitution of H_0 into equation (5b) using equation (13). Thus, the equation for the intermediate lines on Fig. 6 can be explained by

$$(T-T_c)\frac{kA}{H'Qt}=\left(\frac{z}{H'}\right)-\frac{R}{2}\cdot\left(\frac{z}{H'}\right)^2. \quad (14)$$

where R is the ratio of the wall heat to the total heat

$$R=\frac{Q_w}{Q_r+Q_w}. \quad (15)$$

5. CONCLUSIONS

Empirical and analytical formulae have been developed which can be used to explain natural convection in a liquid metal enclosure with floor cooling and heated walls or roof with sufficient accuracy for engineering purposes.

Particular emphasis has been placed on the uniform heated wall case and on defining the temperature profile in the bulk fluid. This is seen to be one-dimensional and is a solution of the steady-state conduction equation involving constant energy generation in the medium. Thus the temperature profile is a conduction gradient, with constant energy generation produced by the convection circulation releasing heat to the conduction mode.

Constant heat flux

The main equation which gives a good prediction of the temperature profile is

$$T^*=z^*-\tfrac{1}{2}(z^*)^2, \quad (5b)$$

where

$$T^*=\frac{kA}{Q_tH_0}(T-T_c)$$

and

$$z^*=\frac{z}{H_0}.$$

This is similar to the Fourier equation for linear conduction, but with an additional function on the right-hand side which accounts for the natural convection induced by the uniformly heated sidewall.

Isolation of the heat distribution into the convection and conduction modes has been made and this enables the convection mass flow induced in the enclosure to be quantified and given by equation (10)

$$m'(z^*)=\frac{\rho\cdot A\alpha}{H_0}\left(\frac{z^*}{1-z^*}\right) \quad (10)$$

and can be solved for values of $z^*<1$.

Boundary layer effect

The influence of the boundary layer is discussed with experimental observation of the extra temperature in this region compared with the local bulk fluid. In sodium this effect is small and represents 2.8% of the total applied wall heat, which gives the appearance of a slightly heated top boundary condition.

Other heat variants

Equation (5b) can be applied to cases involving a heated roof as well as a uniformly heated sidewall. The text discusses further the application of the formulae to this problem and reports the results of tests involving nonuniform wall heating.

Acknowledgements—The permission of NNC Ltd to publish this paper is gratefully acknowledged.

REFERENCES

1. G. Kenworthy, G. L. Quarini, K. H. Winters, N. Sheriff and D. A. Booth, Study of natural convection phenomena in the LMFBR intermediate plenum. *BNES Conference on Liquid Metal Engineering and Technology*, Oxford, UK, Vol. 1, pp. 179–185, April (1985).
2. D. A. Booth, P. A. Glover and N. Sheriff, Natural convection measurements in a mercury-filled rectangular plenum, *Int. J. Heat Mass Transfer* **30**, 1419–1425 (1987).
3. N. Sheriff and N. W. Davies, Liquid metal natural convection from plane surfaces, *Int. J. Heat Fluid Flow* **1** (1979).
4. M. Necati Ozisik, *Heat Transfer*. McGraw-Hill, New York (1985).

APPENDIX A

Solution of the one-dimensional steady-state conduction equation for the natural convection cell involving constant energy generation in the medium.

Assumptions

k(W m^{-1} K^{-1}) = constant thermal conductivity
g_0 (W m^{-3}) = constant energy generation in medium.

Hence

$$\frac{d^2T}{dz}=\frac{g_0}{k}.$$

Boundary conditions

(1) $z=H, \dfrac{dT}{dz}=0$

(2) $z=0, T-T_s$, assume $h=\infty$, i.e. $T(z=0)=T_s$

1st integration

$\dfrac{dT}{dz}=-\dfrac{g_0z}{k}+C_1$, where $C_1=\dfrac{g_0H}{k}$ from the first boundary condition

2nd integration

$T=\dfrac{g_0z^2}{zk}+\dfrac{g_0Hz}{k}+C_2$, $C_2=T_s$ from the second boundary condition

$$Q = g_0 AH \therefore g_0 = \frac{Q}{AH}$$

substitute g_0 into solution of 2nd integration, hence

$$(T - T_\infty) = \frac{QH}{Ak}\left(\left(\frac{z}{H}\right) - \frac{1}{2}\left(\frac{z}{H}\right)^2\right)$$

and

$$\frac{kA}{QH}(T - T_\infty) = \frac{z}{H} - \frac{1}{2}\left(\frac{z}{H}\right)^2$$

i.e.

$$T^* = z^* - \tfrac{1}{2}(z^*)^2 \quad \text{[QED equation (5b)]}.$$